

MODEL 9975 LIFE EXTENSION PACKAGE 2 – FINAL REPORT

W. L. Daugherty

Savannah River National Laboratory
Materials Science & Technology

Publication Date: April 2010

Savannah River Nuclear Solutions
Savannah River Site
Aiken, SC 29808

This document was prepared in conjunction with work accomplished under Contract No. DE-AC09-08SR22470 with the U.S. Department of Energy.

DISCLAIMER

This work was prepared under an agreement with and funded by the U.S. Government. Neither the U. S. Government or its employees, nor any of its contractors, subcontractors or their employees, makes any express or implied: 1. warranty or assumes any legal liability for the accuracy, completeness, or for the use or results of such use of any information, product, or process disclosed; or 2. representation that such use or results of such use would not infringe privately owned rights; or 3. endorsement or recommendation of any specifically identified commercial product, process, or service. Any views and opinions of authors expressed in this work do not necessarily state or reflect those of the United States Government, or its contractors, or subcontractors.

Model 9975 Life Extension Package 2 – Final Report

APPROVALS:

W. L. Daugherty _____ Date _____
Author, Materials Science and Technology

T. E. Skidmore _____ Date _____
Technical Review, Materials Science and Technology

K. A. Dunn _____ Date _____
Pu Surveillance Program Lead, Materials Science and Technology

G. T. Chandler _____ Date _____
Manager, Materials App & Process Tech

E. R. Hackney _____ Date _____
NMM Engineering

REVIEWS:

J. L. Murphy _____ Date _____
Savannah River Packaging Technology

J. W. McEvoy _____ Date _____
9975 Shipping Package Design Authority

Revision Log

Document No. SRNL-STI-2010-00185 **Rev. No.** 0

Document Title Model 9975 Life Extension Package 2 – Final Report

| <u>Rev. #</u> | <u>Page #</u> | <u>Description of Revision</u> | <u>Date</u> |
|---------------|---------------|--------------------------------|-------------|
| 0 | all | Original document | 4/27/2010 |

Summary

Life extension package LE2 (9975-04162) was instrumented and subjected to an extreme temperature environment for 81 weeks. During this time, the maximum fiberboard temperature was ~240 – 250 °F, and was established by a combination of internal heat (19 watts) and external heat. This temperature matches the fiberboard continuous service rating, although such extremes are not expected for normal operation in KAMS.

Several tests and parameters were used to characterize the package components. Results from these tests generally indicate agreement between this full-scale shipping package and small-scale laboratory tests on fiberboard and O-ring samples. These areas of agreement include the rate of fiberboard weight loss, change in fiberboard thermal conductivity, fiberboard compression strength, and O-ring compression set.

In addition, this package provides an example of the extent to which moisture within the fiberboard can redistribute in the presence of a temperature gradient such as might be created by a 19 watt internal heat load. Moisture re-distribution in this package was further exaggerated by a majority of the fiberboard being heated to above the boiling point of water. The majority of water within the fiberboard migrated to the bottom layers of fiberboard, where it contributed to accelerated degradation beyond that expected based solely on the temperature.

Background

This report summarizes information on a 9975 package tested per Task Technical Plan WSRC-TR-2005-00014 [1], which is part of the comprehensive 9975 package surveillance program [2]. This task provides an integrated assessment of the package response to environmental extremes, and demonstrates the extent to which data from small laboratory samples scale up to a full package. The primary goal of this task is to validate aging models currently under development based on lab scale testing of the fiberboard overpack and containment vessel O-rings. A secondary goal is to examine the behavior of the lead shielding under bounding conditions.

Three 9975 packages were modified to provide instrumentation for monitoring package response and performance to environmental aging. Each package has a different environmental exposure history. The second package (LE2, or 9975-04162) was terminated after 81 weeks in test. At this point, the fiberboard was visually degraded, and a significant amount of the moisture originally distributed throughout the fiberboard had accumulated within the bottom ~1 inch of the fiberboard. The stainless steel air shield attached to the upper fiberboard assembly detached, creating difficulties in removing the upper fiberboard assembly from the drum. Additional efforts followed to test the mechanical and thermal properties of the fiberboard, and to characterize the containment vessel O-ring seals. This report documents the test data and conclusions related to test package LE2.

The primary focus of LE2 was to age the fiberboard at its maximum allowable temperature. When this task began, both the KAMS safety basis (for storage) and the SARP (for transportation) accepted the possibility of, and allowed fiberboard temperatures during normal operation up to 250 °F [1]. This value matches the fiberboard continuous service rating, and the maximum

temperature used for aging laboratory samples. Subsequent re-evaluation of KAMS operating conditions and reduction of several conservatisms has resulted in the recognition that the maximum fiberboard temperature will be much lower [3, 4] (i.e. less than the calculated maximum shield temperature of ~200 °F).

Experimental Method

This life extension package is a 9975 shipping package that was modified to add instrumentation and an internal heat source. An access port for fiberboard sample removal and a view port were added to the drum side wall. Thermocouples provide the temperature at a number of locations throughout the package, including the 3013 payload, PCV, SCV, multiple locations within the fiberboard, and drum surface. A sketch showing thermocouple locations is provided in Figure 1.

Package LE2 was placed within an environment with external temperature control, but no humidity control. A cartridge heater inside a modified 3013 container provides 19 watts internal heat. The external temperature was established by enclosing the package in a modified 55 gallon drum, and placing a drum heater around this larger drum (Figure 2). The external blanket heater was adjusted to provide a maximum fiberboard temperature of 240 – 250°F.

The PCV and SCV were modified to allow placement of a cartridge heater through the bottom of the containment vessels and into a well in the 3013. The 3013 was welded shut with a surrogate load of steel shot. The cartridge heater conductors and thermocouples attached to the 3013, PCV and SCV exit the package opposite the side where the fiberboard is instrumented, to minimize disruption of the measured fiberboard thermal profile.

The modifications to the PCV and SCV provided open penetrations in the bottom of each vessel. Because of this, both O-rings in each vessel can receive a sensitive helium leak test. Normally, only the outer O-ring is leak-tested with a helium detector, which provides assurance of a leak-tight seal of 1×10^{-7} std cc air/sec (or 2×10^{-7} std cc He/sec). After loading the package, the leak-tightness of both O-rings is confirmed at a level of $\sim 1 \times 10^{-3}$ std cc air/sec with a less sensitive rate of pressure rise technique. With the modified vessels of LE2, the more sensitive helium leak test can be performed at any time.

Package LE2 was initially brought to temperature slowly and incrementally, to avoid an overshoot in fiberboard temperature. It is likely that during this time (~34 days to reach a fiberboard temperature of 235°F) that significant moisture redistribution was occurring. Most of the moisture in the fiberboard would migrate to the cooler regions of the package (i.e. to the bottom of the package). This in turn would decrease the thermal conductivity for the bulk of the fiberboard, and increase the temperature gradient across the fiberboard.

Thermocouple data from the package is automatically recorded at preset intervals. Additional data is collected on an occasional basis during periodic examinations. This includes:

- Photographs of the fiberboard position through the view port
- Weight of the entire package
- Weight and moisture content of the removable fiberboard sections
- Visual observations of the package exterior

- Weight and dimensions of the fiberboard assemblies and shield
- Visual observations of other package components

The last 2 of the above data sources require opening the drum lid and removing internal components. These steps are not performed with every examination, so these data are not collected as often as the other items listed.

Results – Periodic Data

There are several metrics which provided evidence of change in the package over time. These include package weight, fiberboard position within the view port, and the temperature profile across the fiberboard. Additional indications of change might be seen in the weight and appearance of the fiberboard, dimensional variation of the lead shield, and from visual observations of the components.

Significant changes in LE2 were observed during the early inspections. Indications of change noted after 9 weeks in test (~3 weeks at temperature) without opening the package included:

- The bottom fiberboard layers (~ 1 inch) of the removable fiberboard sections were saturated with water, and very little moisture remained in the fiberboard above.
- The fiberboard shrank axially, evidenced by a drop of ~3/4 inch at the view port.

The package was first opened after 19 weeks in test, with additional observations of significant change, as follows:

- Stains from the drying of liquid water remained on the underside of the drum lid and the top of the components immediately below the lid. (Figure 3)
- Additional axial shrinkage of the fiberboard produced an axial drop at the view port of ~1 inch.
- Significant corrosion was observed on the shield. (Figure 4)
- Dark stains were observed on the fiberboard ID surface (apparently related to shield corrosion). (Figure 5)

A plot of package weight over time is shown in Figure 6. The weight of the upper fiberboard assembly was also tracked over time, although it was recorded less frequently. These data are shown in Figure 7. Two small sections of fiberboard were cut from the bottom of the lower assembly, and are accessible to remove through a hatch on the drum side. These sections are characterized more often than the drum is opened to inspect the upper or lower fiberboard assembly. Weight data for these removable sections are shown in Figure 8. Their moisture content is summarized in Table 1.

Photographs of the removable sections help to track fiberboard changes over time. A sequence of these photographs is shown in Figure 9.

With test LE2, the bottom layers of the removable sections (as well as the rest of the lower fiberboard assembly) darkened significantly as they accumulated excess moisture. The bottom layers were observed to be saturated during the first inspection (after 3 weeks at temperature, 8 weeks total exposure), and a strong odor of decaying vegetation was noted after 19 weeks in test.

A steep moisture gradient existed at the bottom of LE2; the saturated layers had a moisture content of 100 %WME, while approximately ½ inch above this region the moisture content was typically 17 %WME or less. The temperature of the removable sections within the conditioning environment was not recorded.

The drum was modified to include a view port on the side. A pattern was marked on the lower fiberboard assembly to be viewed through the view port, and identify the extent to which the fiberboard moved. Typical photographs of this pattern through the view port are shown in Figure 10. As observed through the viewport, the overall fiberboard height was reduced, as indicated by the pattern shifting downward. Measurements were made from photographs taken at each inspection interval to estimate the amount of fiberboard movement. These measurements are summarized in Figure 11.

After 19 weeks in test (96 days at temperature), dimensional measurements were made on test 2 to determine whether an axial gap had opened between the upper and lower fiberboard assemblies. At this time, the fiberboard visible at the upper edge of the window had dropped by 0.98 inch. Calculations indicated that a vertical gap of approximately 0.6 inch existed between the two assemblies, but this value is based on assumptions regarding the uniformity of shrinkage over the height of each assembly. Both fiberboard assemblies and the shield were measured after 81 weeks exposure. Based on these final measurements, a vertical gap of 1.19 inches had opened between the two assemblies. The fiberboard had dropped a total of 1.8 inches at the top edge of the window at this time.

Given the relatively low melting temperature of lead (621°F), the shield may experience creep at service temperatures. Measurements of the LE2 shield were analyzed to investigate this possibility, and are summarized in Table 2.

The corrosion of the lead shield is also of interest. In LE2, the corrosion product was observed during the first inspection, after 19 weeks in test, and was dark gray / black and nodular (Figure 4). This is in sharp contrast to the corrosion typically seen on a 9975 shield (smooth white surface). Chemical analysis of corrosion product collected from LE2 showed that it was generally consistent with the lead carbonate seen on other packages. However, elevated levels of chlorine (varies between ~2 to 10 wt%) were also present. Although unconfirmed, the chlorine most likely leached from the fiberboard. Figure 12 shows the appearance of the shield at the end of testing. With little obvious change in appearance since week 19, it is likely that most of the shield corrosion occurred in the first few weeks of test when significant moisture re-distribution was occurring.

Twelve thermocouples monitor the temperature gradient within the fiberboard. The hottest measured temperature within the fiberboard is at the highest thermocouple elevation on the ID surface, and the coolest measured temperature within the fiberboard is at the lowest thermocouple elevation on the OD surface. The temperature vs time data at the highest fiberboard ID and lowest fiberboard OD locations are summarized in Figure 13. It is possible that the fiberboard reached slightly higher temperatures at elevations above the uppermost ID thermocouple. However, the variation among the 4 thermocouples along the ID surface in the central region adjacent to the shield shows a modest gradient (~6°F). Therefore, the recorded temperatures are assumed to provide a reasonable approximation of the maximum fiberboard conditions.

Along the OD surface, the four thermocouples indicate a vertical gradient approximately 5 times steeper than along the ID surface. The degree of excess moisture at the bottom of the package suggests that a relatively steep temperature gradient exists within the bottom several inches.

The package experienced a number of temperature transients associated with inspections, power outages, etc. In between these transients are periods of relatively steady state operation. To better illustrate possible changes of the fiberboard thermal properties, the fiberboard temperature profile is examined at select periods of steady state operation. The temperature profile across the sidewall of the fiberboard is plotted in Figure 14.

Results – Final Inspections

Based on the degradation of LE2 fiberboard and the air shield becoming detached from the upper fiberboard assembly after 81 weeks in test, it was decided that the package would not return to test. Accordingly, the LE2 SCV and PCV received a final leak test, and each vessel was opened to examine the O-rings. Destructive tests were performed on the lower fiberboard assembly and the PCV inner O-ring. The leak test on each containment vessel interrogated both O-rings, and the measured leak rate met the acceptance criterion of $<2.0 \text{ E-7 std cc He/sec}$. O-ring measurements were taken following several time intervals after the vessels were opened. The first measurements are based on photographs of the O-rings still installed on the cone seal plug taken 5 minutes after opening. Subsequent measurements were taken with a snap gage after the O-rings were removed, at periods of <30 minutes, 9 days and 30 days after opening. Compression set of each O-ring is calculated based on each of these measurement periods. Results are summarized in Table 3.

The PCV inner O-ring also received a final dimensional characterization 189 days after removal, prior to destructive testing. At this time, the compression set was 31%, showing little change from the previous 30 day measurement (Table 3). The PCV inner O-ring was then tensile tested as a single strand sample. There was sufficient length to obtain two test samples. The stress-strain curves are shown in Figure 15, compared to a baseline (non-aged) O-ring. The ultimate strength and elongation of both samples are higher than those of the baseline sample. This is typical of O-rings tested to date following service [5], and may reflect a weaker than nominal baseline O-ring.

Following tensile testing, a small portion of the PCV inner O-ring was subjected to dynamic mechanical analysis (DMA) testing. While this technique can identify a number of characteristics of the polymer material, the primary objective of this test was to determine whether the glass transition temperature (T_g) had changed as a result of the conditioning history. An increase in T_g could signal a decreased ability to maintain a leak-tight seal at low temperatures. As a comparison, DMA testing was also performed on a non-aged O-ring, and an O-ring that experienced elevated temperature (300°F) for 654 days, followed by an extreme temperature excursion ($>720^\circ\text{F}$). The DMA shows no significant difference in T_g among the three samples, with results ranging from -27.7 to -28.6°C (Figure 16).

Samples were removed from the lower fiberboard assembly for thermal conductivity, specific heat capacity and compression testing. During cutting, it was noted that the sidewall material (above the lower bearing plate) was very soft, and cut easily with a hand saw. Rather than the typical

release of recognizable fibers, cutting produced a fine powder. In contrast, the bottom layers of fiberboard (below the lower bearing plate) displayed progressively less damage, with three distinct regions (see Figure 17). The bottom region appears similar to undegraded fiberboard, and is typically $\frac{1}{2}$ - $\frac{3}{4}$ inch thick. The upper region is darkened, and appears somewhat weakened, but retains distinct fibers. The middle region is heavily darkened, and is much harder than undegraded fiberboard. It appears to have a significant quantity of embedded particulate material, and is suggestive of leachable material deposited at a “high water” mark. This middle region is thickest around the outside perimeter, and decreases towards the fiberboard interior.

A section of fiberboard from the middle region near the bottom was examined in the scanning electron microscope, to determine its elemental composition. Each of 5 distinct layers was analyzed (Figure 18). Most of the ingredients in the fiberboard (cellulose, starch, paraffin wax and wood glue) are composed of carbon, hydrogen and/or oxygen compounds. In addition, clay can include aluminum, silicon and other mineral compounds.

During the period between package conditioning and removing the fiberboard test samples, the moisture gradient in the fiberboard diminished significantly. The moisture content of the bottom layers had dropped from ~ 100 % WME to $\sim 14 - 16$ % WME, while the moisture content of the sides increased from < 6 % WME (the moisture meter will not register below this value) to $\sim 7 - 8$ % WME. The thermal conductivity and compression test samples removed from the upper sidewall of the lower assembly were placed in a 185°F oven for several hours to reduce their moisture content prior to testing. The thermal conductivity samples and three of the five compression test samples removed from the bottom were tested as is. Testing thermal conductivity samples with high moisture levels is problematic due to the active migration of moisture under a thermal gradient. The impact of the reduced moisture level on compression strength was addressed by placing the remaining two compression samples in shallow standing water to re-create a moisture content similar to that during conditioning. The bottom $\sim 1/2$ inch of each sample became saturated, while the moisture content of the top layer increased to ~ 17 % WME. These two samples were tested in the two orientations (one parallel and one perpendicular).

Results of the compression tests are shown in Figures 19 and 20, for the parallel and perpendicular orientations, respectively. Metrics from these tests which provide a basis to draw sample-to-sample comparisons are summarized in Table 4. The buckling strength (applicable only to parallel orientation samples) is the stress at which the fiberboard layers begin to buckle. The area under the stress-strain curve up to 40% strain provides a relative indication of the energy absorption capability of the sample.

Results of the thermal conductivity testing are summarized in Table 5. Small scraps from the upper sidewall of the lower fiberboard assembly were collected and placed in a capsule to measure the specific heat capacity. At a mean temperature of $\sim 125^{\circ}\text{F}$, the measured specific heat capacity is 1300 J/kg-K. This value is the average of 6 trials, conducted in accordance with ASTM C351. The specific heat capacity measured on other 9975 packages that were destructively examined ranged from $1300 - 1875$ J/kg-K. Since the LE2 fiberboard sample was relatively dry, and the specific heat capacity increases with moisture content, this result for aged LE2 fiberboard material is consistent with that from the other packages.

Discussion

The LE2 environment approximates the continuous service rating for the fiberboard temperature, but is much hotter than expected in KAMS. When the package was at the target temperature (maximum recorded fiberboard temperature of 240 – 250°F), all but one thermocouple within the fiberboard indicated a temperature above the boiling point of water. The one exception was the lowest thermocouple on the fiberboard OD surface, which typically read 190 – 200°F. This indicates the large majority of fiberboard held no free liquid throughout most of the test. It is likely that several key changes within the package (such as shield corrosion and the initial fiberboard shrinkage and weight loss) occurred during the initial heatup.

During the last inspection, package LE2 had the air shield detach from the upper fiberboard assembly. It detached with very little force as the assembly was being removed from the package. Several wire hooks were improvised to pull the upper fiberboard assembly from LE2, leaving significant impressions in the degraded fiberboard. The air shield is attached to the fiberboard with silicone adhesive. Upon separation, some adhesive remained on the fiberboard, while most separated with the air shield. A region of the silicone on the air shield also had fiberboard still attached. This dual behavior (fiberboard remaining on the silicone, and silicone still attached to the fiberboard, see Figure 21) indicates that failure of both the fiberboard and silicone contributed to the separation.

Thermal conductivity changes for package LE2 vs laboratory data

Package LE2 data were examined for evidence of change in fiberboard thermal conductivity during the testing. There is a region of relatively constant thermal response among the upper 3 thermocouples on the fiberboard ID and OD surfaces. The temperature along either surface varies little within this region during steady state operation. This region will be the primary focus in examining any change in thermal properties. Since some heat is lost through the top and bottom of the package, the heat conducting through this side region will be less than 19 watts, but it will be assumed constant over time. Heat conduction in this region is in the radial orientation.

Thermal gradient information was examined at several discrete times during periods of steady state operation indicated by the arrows in Figure 22. The thermal conductivity will vary with changes in the temperature gradient and fiberboard thickness, as described by:

$$q/A = k * \Delta T / t$$

where, q/A = heat flux (assumed constant)

k = thermal conductivity

ΔT = radial temperature gradient

t = lower assembly radial thickness (linear interpolation based on available inspection data)

At each of the arrows in Figure 22, the radial temperature gradient and lower assembly thickness are combined per this relationship to get a value proportional to the thermal conductivity (see Table 6). Any change in this value over time is proportional to the change in actual thermal conductivity. (Since the actual heat flux through this region of fiberboard is unknown, the actual thermal conductivity cannot be calculated directly.)

In Reference 6, the value at the first arrow in Figure 22 (at 52 days in test, 18 days at temperature) was taken as a reference point, and the values for subsequent data points show the change in thermal conductivity relative to this first data point. This produced the curve shown in Figure 23, which shows a net decrease over time comparable to that seen in laboratory samples conditioned at 250°F. Further review suggests that the assumption of constant heat flux might not be valid for the first data point (52 days in test), based on the following:

- The ratio between radial heat flux (through the package sides) and axial heat flux (through the package top and bottom) can change as the thermal conductivity changes in these regions. The thermal conductivity in each region will change as the moisture content changes.
- Significant moisture decrease likely occurred in each region of the fiberboard as the local temperature approached and increased past ~212°F, such that any liquid water would boil off, and re-distribute to cooler regions. The fiberboard ID surface first reached 212°F after 15 days in test. The last 2 fiberboard thermocouple locations reached this temperature after 42 days and 63 days in test, respectively.
- A further one-time change to the heat flux distribution within the package occurred after 42 days in test, when additional insulation was added around the top and bottom of the 55-gallon drum that contained LE2.

The second arrow in Figure 22 represents approximately 99 days in test (64 days at temperature). The data from this point and later are expected to better meet the assumption of constant heat flux. Accordingly, the relative change in thermal conductivity values were re-normalized to the second value after 64 days at temperature. These results are listed in Table 6 and plotted in Figure 24, along with normalized laboratory data for samples conditioned at 215 (sample 00826R) and 250°F (sample 2234-R) and tested at 185°F. In this presentation, the relative thermal conductivity values for LE2 show a decrease with time, and fall between the trends for the two laboratory samples. This intermediate behavior for LE2 is consistent with the estimated average sidewall temperature of ~235°F, which falls between the conditioning temperatures of the two laboratory samples.

Fiberboard thermal conductivity can change due to change in the moisture content, or from fiberboard degradation. The above exercise indicates a decrease in radial thermal conductivity of the fiberboard sidewall of ~18% compared to the conductivity after 18 days at temperature. At this point (18 days at temperature), the sidewall would have lost much of its moisture, and the 18% decrease can be attributed primarily to fiberboard degradation. Based on the sample removed from that location, the measured radial thermal conductivity is 0.0862 W/m-K at a mean temperature of 185°F. Radial thermal conductivity laboratory samples conditioned in ovens at 185°F and higher (and therefore retaining very little moisture) had initial conditioned thermal conductivity values of 0.922 – 0.1175 W/m-K, with an average value of 0.1023 W/m-K. The initial thermal conductivity of the LE2 lower fiberboard assembly is unknown. However, if an 18% decrease is combined with the measured post-test value of 0.0862 W/m-K, then the initial “dry” thermal conductivity for the LE2 fiberboard sidewall was 0.105 W/m-K. This is in good agreement with the range of laboratory samples.

Fiberboard mass changes vs lab data

Variation in the total weight of the package is summarized in Figure 6. Variation in the weight of the upper fiberboard assembly and the removable fiberboard sections is shown in Figures 7 and 8,

respectively. It is assumed that the change in package weight is associated with the fiberboard alone (ignoring effects of weight gain from the shield corrosion). It is further assumed that there was no significant moisture loss from the package following the initial heatup. This assumption is based on the observation that the bottom (larger) removable fiberboard section did not change weight significantly after the initial re-distribution of moisture to the bottom (Figure 8), and no significant moisture remained anywhere else within the package.

The package as a whole lost weight at an average rate of 0.004% /day. The package contains 32.156 kg of “dry” fiberboard (based on the initial weight of both fiberboard assemblies and removable sections, minus the weight of bearing plates and air shield, minus the initial package weight decrease due to moisture loss). Accordingly, the overall average rate of fiberboard weight loss is 0.022 %/day, or 7.9 %/yr. Similarly, using the data from Figure 7, the average fiberboard weight loss rate for the upper assembly is 0.028 %/day (10.4 %/yr). The average weight loss for the small (upper) removable fiberboard section is 0.012 %/day (4.4 %/yr).

The average fiberboard temperature at the higher elevations (near the upper assembly) is estimated to be close to 235°F, and the temperature near the bottom of the package is likely significantly cooler than 190°F (based on the steep moisture gradient and the coolest fiberboard thermocouple reading of ~190 – 200°F). Therefore, a typical median temperature would be ~215°F.

In comparison to the LE2 fiberboard data, laboratory samples conditioned at 215°F lost weight at an average rate of ~0.01 %/day (3.6 %/yr), while samples conditioned at 250°F lost weight at an average rate of ~0.04 %/day (15 %/yr) [7]. These values are generally consistent with the behavior of LE2.

Fiberboard Strength Changes vs Laboratory Data

Some variation is seen in the compressive strength of the LE2 fiberboard samples for both test orientations (Figures 19, 20). A greater degree of variation is seen between these samples and undegraded fiberboard. Figures 25 and 26 compare these compression data with several laboratory samples, for the two test orientations. Comparative metrics for the various conditions are summarized and compared to laboratory samples in Table 4.

Samples tested with the load applied parallel to the fiberboard layers are compared in Figure 25. (This orientation is relevant to a side impact scenario, such as a forklift impact.) All the LE2 samples are significantly weaker than baseline (non-aged) samples. The LE2 sample from the side region is similar to laboratory samples aged at 250°F for 64 weeks. The LE2 sample from the base with elevated moisture is similar overall to laboratory samples aged 64 weeks at 215°F. The key difference is that the LE2 sample has a lower initial buckling strength. The LE2 sample from the base with a reduced moisture content regained some strength relative to the elevated moisture condition, but this sample is still significantly weaker than the baseline sample.

Samples tested with the load applied perpendicular to the fiberboard layers are compared in Figure 26. Similar to the parallel orientation, the perpendicular LE2 samples are consistent with laboratory samples aged at 250°F for 64 weeks. In contrast, the base LE2 samples with reduced moisture content are comparable to laboratory samples aged 64 weeks at 215F, and show no

significant difference from non-aged samples. The LE2 base sample with elevated moisture, however, is weaker than the base sample with reduced moisture.

Potential for Shield Creep

The data in Table 2 indicate the possibility that creep of the lead shield occurred in LE2, although this conclusion is complicated by the fact that the shield dimensions were also changing due to corrosion. Creep of the lead would be manifested by a reduction in wall thickness at the top of the shield, and an increase in wall thickness near the bottom. The observed corrosion on the shield was generally uniform over the entire surface.

At the top of the LE2 shield, the average radial thickness remained relatively constant (maximum increase of 0.008 inch). In the absence of creep, it would be expected to increase due to the accumulation of corrosion product. In contrast, the average radial thickness at the bottom increased by 0.032 – 0.034 inch. Corrosion alone would be expected to produce a similar increase in shield thickness at the top and bottom. It is not obvious why the measured radial thickness (at either top or bottom) is greater after 36 weeks than after 81 weeks, but this may reflect measurement uncertainty.

Using the shield measurements after 81 weeks, if the loss in wall thickness at the top due to creep is assumed equal to the increase in wall thickness at the bottom due to creep, then a change in thickness of ~0.014 inch at each location can be attributed to creep, while corrosion has led to a uniform increase in thickness of ~0.018 inch. This would correlate to a rate of $(0.014 * 52/81 =)$ 0.009 inch/year change in thickness due to creep. If the shield measurements taken at 36 weeks were used instead, the data would indicate a creep rate of $(0.013 * 52/36) = 0.02$ inch/year.

Literature data can be used to estimate the potential for lead creep based on the temperature and stress in the shield. In LE2, the fiberboard ID surface was typically 240 – 245°F. Accordingly a typical shield temperature of 250°F (394K) will be assumed. With a melting temperature of 621°F (601K), the shield homologous temperature (temperature / melting temperature) is 0.66. The stress in the shield is primarily from its own weight. The stainless steel liner will be assumed to carry the weight of the upper fiberboard assembly. It will also provide some reinforcement to the lead, but this effect will be ignored for now. With a shield height of ~24.7 inches, the stress on the shield at a height 1 inch from the bottom will be:

$$\text{Stress} = 23.7 \text{ in} * (708 \text{ lb/ft}^3) / (12 \text{ in/ft})^3 = 10 \text{ psi} (=0.07 \text{ MPa})$$

This value corresponds to a shear stress of 0.04 MPa. With a shear modulus of 7300 MPa for lead at 300K, the normalized shear stress is $(0.04 / 7300 =)$ 5 E-6. Reference 8 provides a map of lead creep rates as a function of normalized shear stress and homologous temperature for grain sizes of 10 μ and 1 mm. The grain size of the shield likely falls between these two values. The map indicates a creep rate of 7 E-9 /sec for a grain size of 10 μ, and ~1 E-11 /sec for a grain size of 1 mm. For the finer grain size, this creep rate converts to 22%/year, or 0.11 inch/year. For the larger grain size, the shield creep rate would be negligible (~0.0002 inch/year). The actual creep rate likely falls between these two values, as suggested by the estimates based on shield measurement data.

LE2 O-Rings

The O-rings in LE2 were generally at a temperature of ~265°F (PCV) or ~255°F (SCV), with a total time at temperature of 461 days. This is lower than the O-ring continuous service rating (300°F for up to 10 years in KAMS), but significantly higher than actual O-ring temperatures in KAMS (198 °F maximum during normal operation) [9].

The compression set measured initially upon opening ranged from 58 to 67%. These values are based on measurements taken from photographs of the O-rings still installed on the cone seal plug. Thickness measurements were taken with a snap gage approximately 20 minutes later, giving slightly smaller, but comparable, values. This illustrates the validity of measurements from photographs, which can provide an opportunity to obtain data sooner after opening a vessel. After 30 days, the compression set values had decreased to a range of 26 to 45%. Re-measuring the PCV inner O-ring 189 days after removal showed little additional change in the compression set.

Data from laboratory testing of O-rings [10] indicates that the compression stress relaxation for a similar exposure (250°F for 461 days) would be ~50%. While compression set and compression stress relaxation do not necessarily change at the same rate for a given environment, this comparison does illustrate a degree of consistency between package LE2 and laboratory data.

The Viton ® O-rings are rated for service at a minimum temperature of -40°F, although aged O-rings have not been tested to verify their performance at this condition. While temperatures this low are not of concern for storage in KAMS, shipping packages are required to maintain a leak-tight seal to temperatures as low as -40°F during transport. With the measured glass transition temperature (-28°C, or -18°F) above this value, performance of the O-rings at -40°F could be sensitive to relatively minor changes from aging. However, there was no significant difference in T_g between the aged and baseline O-rings. Therefore, the molecular changes that might typically produce changes in T_g were not active at the aging conditions experienced by the LE2 O-rings. Note, however, that this does not eliminate the possibility of other aging mechanisms that might impact low temperature performance. Certainly, the O-rings experienced a significant compression set, indicating physical changes within the O-ring.

Conclusions

Life extension package LE2 has been instrumented and exposed to a bounding storage condition to help identify the extent to which laboratory test results for fiberboard, O-rings and other components apply to a full-scale package. Results to date indicate the following:

- With elevated temperature, the fiberboard loses mass (due to pyrolysis) and shrinks. Shrinkage is greatest in the axial direction. This behavior is consistent with laboratory samples.
- The fiberboard thermal conductivity decreases over time at elevated temperature. Estimates of the change in thermal conductivity (in the radial direction) are consistent with changes seen in laboratory samples. These estimates also suggest that the radial thermal conductivity was initially similar to an average value observed in non-aged laboratory samples.
- The fiberboard compression strength was degraded to an extent comparable to laboratory samples aged under similar conditions. The elevated moisture in the bottom fiberboard layers

- further reduced the compression strength. Some of this strength loss is recovered as the moisture level is reduced. A similar partial recovery is seen in laboratory samples.
- The lead shield experienced significant corrosion, with the morphology differing from that typically seen in 9975 packages. However, analysis of the corrosion product identified a composition consistent with the lead carbonate observed on other packages. The primary difference in composition was the additional presence of chlorine in the LE2 sample.
 - Based on laboratory test data on O-rings to date, failure of the O-rings is not expected for the conditions experienced by LE2. The O-rings in the LE2 containment vessels remain leak-tight. Upon opening the LE2 containment vessels, the compression set measured initially was ~58% for the PCV and ~64% for the SCV. These values are similar to the predicted compression stress relaxation based on laboratory data, and indicate the continued capability to maintain a leak-tight seal.

The re-distribution of moisture within the fiberboard can be significant in the presence of a thermal gradient such as that created by a 19 watt internal heat load. In the case of this package, the majority of moisture migrated to the bottom layers of fiberboard, and remained there for the duration of testing. This effect falls beyond the observations of laboratory samples, since those samples typically had no thermal gradient, and no effort was made to simulate the degree of moisture containment provided by the 9975 drum. Parallel efforts are underway to better understand the implications of elevated moisture levels on package performance.

References

- [1] WSRC-TR-2005-00014, Rev. 2, "Task Technical and Quality Assurance Plan for Full-Scale Testing of Model 9975 Packages to Support Life Extension Model Development (U)", June 2008.
- [2] WSRC-TR-2001-0286, Rev. 2, "SRS Surveillance Program for Storage of Pu Material in KAMS".
- [3] WSRC-SA-2002-00005, Rev. 3, "K-Area Complex Documented Safety Analysis", April 2009.
- [4] SRNS-TR-2008-00290, "Summary and Matrix: 9975 Shipping Package Qualification Program for Extended Storage of Plutonium in the K-Area Complex", J. A. Radder, November 2008
- [5] SRNL-STI-2009-00763, "Destructive Examination of Shipping Package 9975-02028", W. L. Daugherty and T. M. Stefek, December 2009.
- [6] SRNL-TR-2009-00439, Rev. 1, "First Interim Status Report: Model 9975 Life Extension Package Testing", W. L. Daugherty and T. M. Stefek, January 2010.
- [7] SRNL-SCS-2008-00062, "Statistical Analysis Fiberboard Density, Weight & Dimensions Test Results", S. P. Harris, October 10, 2008.

- [8] “Deformation-Mechanism Maps, The Plasticity and Creep of Metals and Ceramics”, H. J. Frost (Dartmouth College) and M. F. Ashby (Cambridge University), web version <http://engineering.dartmouth.edu/defmech/>.
- [9] M-CLC-K-00727, “Thermal Model Study for the 9975 Package in KAMS During Facility Fire”, N. K. Gupta, June 11, 2008.
- [10] SRNS-TR-2009-00259, “Lifetime Prediction for Model 9975 O-Rings in KAMS”, E. N. Hoffman and T. E. Skidmore, November 2009.

Table 1. Moisture content of LE2 removable fiberboard sections

| Time at Temp (days) | Moisture Content * (% WME) | * Moisture content (when measured) was typically measured at several elevations along the OD surface of the removable sections. The range reported reflects the measurements closest to the bottom of the lower section (1 st value) and closest to the top of the upper section (2 nd value). |
|---------------------|----------------------------|--|
| 0 | NA | |
| 96 | 100 - <6 | |
| 118 | 100 - <6 | |
| 199 | 100 - <6 | |
| 237 | 100 - <6 | |
| 363 | 100 - <6 | |
| 396 | 100 - <6 | |
| 452 | 100 - <6 | |

Table 2. Dimensional measurements of LE2 shield to investigate the potential for lead creep.

| Time of Measurement | Avg Radial Thickness at Bottom of Shield (inch) | Avg Radial Thickness at Top of Shield (inch) | Difference (Bottom – Top) (inch) |
|---------------------|---|--|----------------------------------|
| Baseline | 0.540 | 0.542 | -0.002 |
| After 36 wks | 0.574 | 0.550 | +0.024 |
| After 81 wks | 0.572 | 0.546 | +0.026 |

Table 3. Compression set data for LE2 O-rings after 81 weeks in test

| Interval between opening vessel and O-Ring measurements | O-Ring Compression Set | | | |
|---|------------------------|------------------|------------------|------------------|
| | PCV Inner O-Ring | PCV Outer O-Ring | SCV Inner O-Ring | SCV Outer O-Ring |
| 5 minutes | 58% | 58% | 67% | 60% |
| 24 minutes | 57% | 54% | 54% | 57% |
| 9 days | 36% | * | 41% | 30% |
| 30 days | 33% | 40% * | 45% | 26% |
| 189 days | 31% | NA | NA | NA |

* This O-ring twisted upon removal. Measurements taken at 9 and 30 days were not consistently in the as-installed radial direction. The value reported at 30 days is based on re-measurement performed at 65 days.

Table 4. Comparative metrics from fiberboard compression tests

| Sample | Buckling Strength (psi) | Area under Stress-Strain Curve to 40% Strain | Sample | Area under Stress-Strain Curve to 40% Strain | Comment |
|--------------------------------|-------------------------|--|----------------------------------|--|---|
| Parallel Orientation | | | Perpendicular Orientation | | |
| LE2 Side 1 | 83 | 14 | LE2 Side 3 | 17 | Low moisture re-established pre-test |
| LE2 Side 2 | 77 | 14 | LE2 Side 4 | 19 | |
| LE2 Base 1 | 132 | 28 | LE2 Base 3 | 43 | Moisture content reduced after conditioning |
| LE2 Base 2 | 157 | 29 | | | |
| LE2 Base 4 | 68 | 17 | LE2 Base 5 | 19 | Elevated moisture content re-established pre-test |
| | | | | | |
| Lab Sample Data for Comparison | 49 - 71 | 9 - 11 | Lab Sample Data for Comparison | 15 - 16 | Conditioned 64 wks at 250°F |
| | 111 - 219 | 24 - 33 | | 27 - 48 | Conditioned 64 wks at 215°F |
| | 152 - 357 | 36 - 78 | | 25 - 61 | Non-aged material |

Table 5. Thermal conductivity data for LE2 fiberboard lower assembly

| Sample Location & Orientation | Thermal Conductivity (W/m-K) for a mean temperature of: | | |
|-------------------------------|---|--------------|--------------|
| | 25°C (77°F) | 50°C (122°F) | 85°C (185°F) |
| Upper side wall, axial | 0.0481 | 0.0503 | 0.0576 |
| Upper side wall, radial | 0.0790 | 0.0821 | 0.0862 |
| Bottom layers, axial | 0.0716 | 0.0801 | (0.0653) * |
| Bottom layers, radial | 0.1297 | 0.1336 | (0.1175) * |

* These two results are inconsistent with the remaining data, in that the thermal conductivity typically increases as the temperature increases. This anomaly is likely due to the relatively high moisture content of these samples, and the lack of an equilibrium moisture gradient during testing.

Table 6. LE2 data used to estimate changes in fiberboard radial thermal conductivity

| Time at Temp. (days) | Avg Fiberboard ID Temperature (°F) | Avg Fiberboard Radial Temp. Gradient, ΔT (°F) | Fiberboard Radial Thickness, t (inch) | $\Delta T / t$ (°F/inch) | Normalized Thermal Conductivity, $4.829 / (\Delta T / t)$ |
|----------------------|------------------------------------|---|---------------------------------------|--------------------------|---|
| 18 | 247 | 21.58 | 4.822 | 4.475 | 1.079 |
| 64 | 242 | 23.27 | 4.819 | 4.829 | 1.000 |
| 188 | 245 | 24.53 | 4.813 | 5.097 | 0.947 |
| 321 | 246 | 24.16 | 4.789 | 5.045 | 0.957 |
| 348 | 241 | 24.65 | 4.784 | 5.153 | 0.937 |
| 450 | 241 | 26.09 | 4.768 | 5.472 | 0.882 |

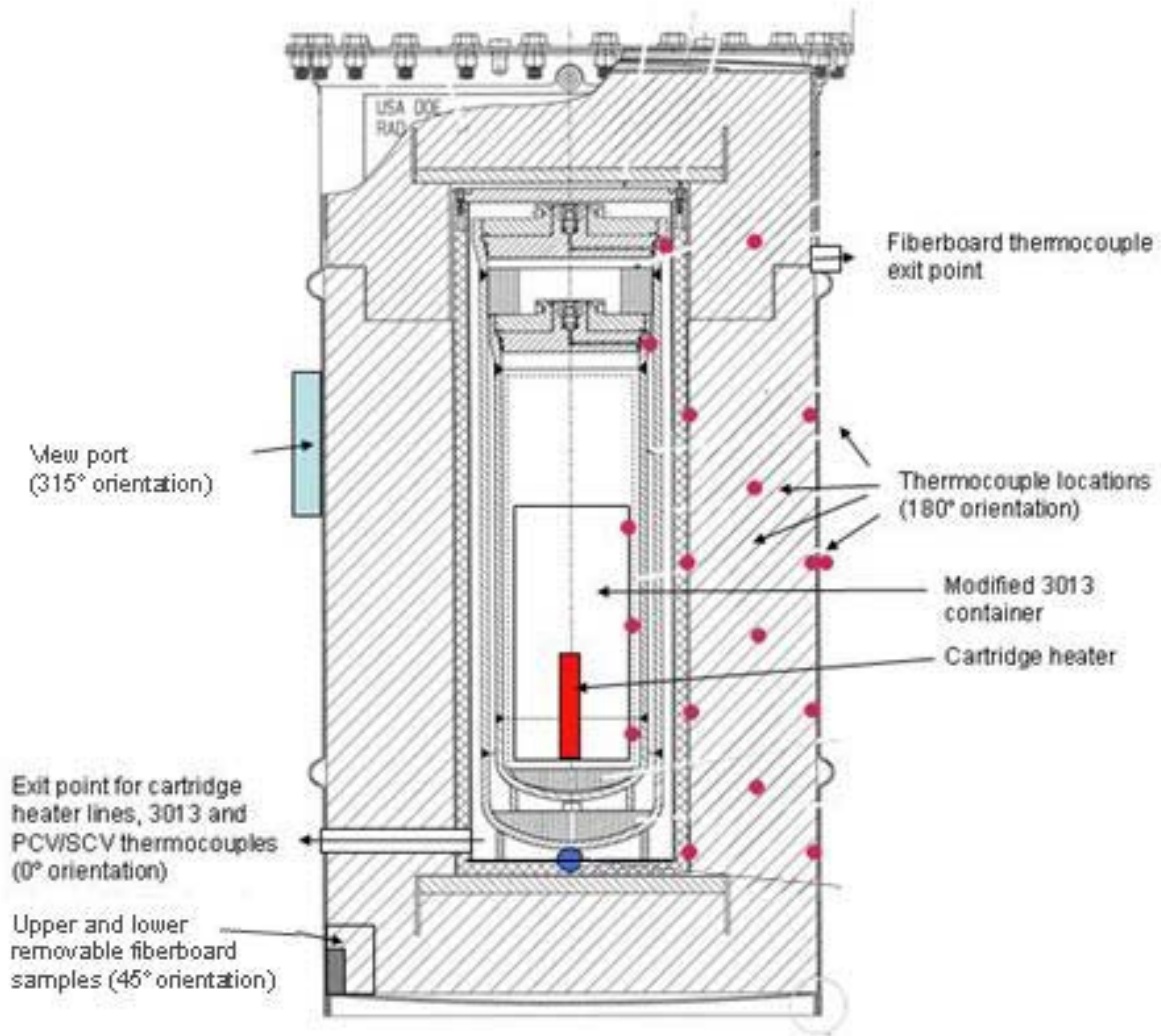


Figure 1. Cross section of 9975 package, showing added instrumentation and examination features.



(a) (b)
Figure 2. Configuration of LE2 to provide external heat source. In (a) LE2 is seen with insulation on top, inside the modified 55-gal drum. In (b), the 55-gal drum is wrapped with a drum heater and insulation.



Figure 3. Stain on LE2 lid and other upper components from initial condensation activity, observed after 19 weeks in test.



Figure 4. Corrosion product on the LE2 shield, after 19 weeks in test.



Figure 5. ID surface of upper fiberboard assembly, showing stains apparently from shield corrosion product after 19 weeks in test.

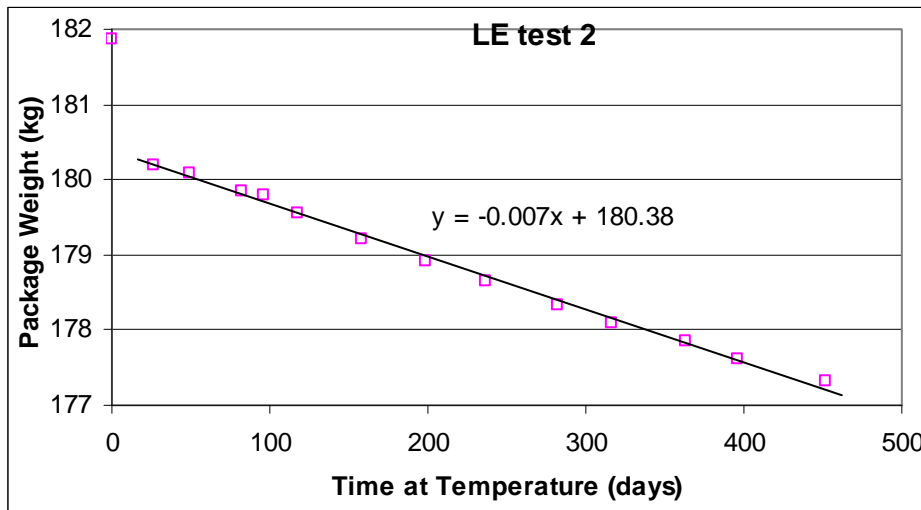


Figure 6. Package weight of LE2 over time. The variation following the initial drop is approximated well by the linear trendline. The magnitude of the initial drop represents moisture loss.

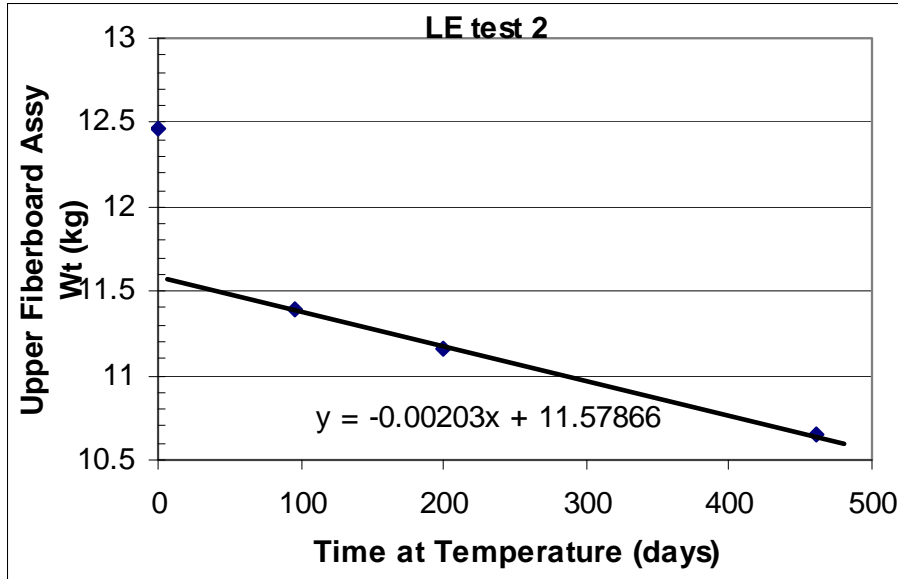


Figure 7. Weight variation for LE2 upper fiberboard assembly.

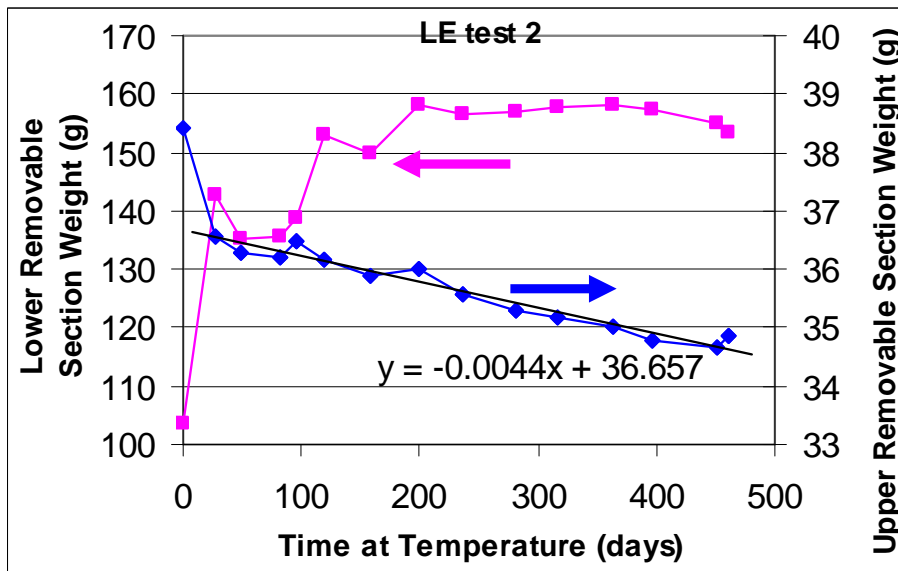


Figure 8. Weight of removable fiberboard sections from life extension test 2.



(a) baseline



(b) 9 wk



(c) 19 wk



(d) 42 wk

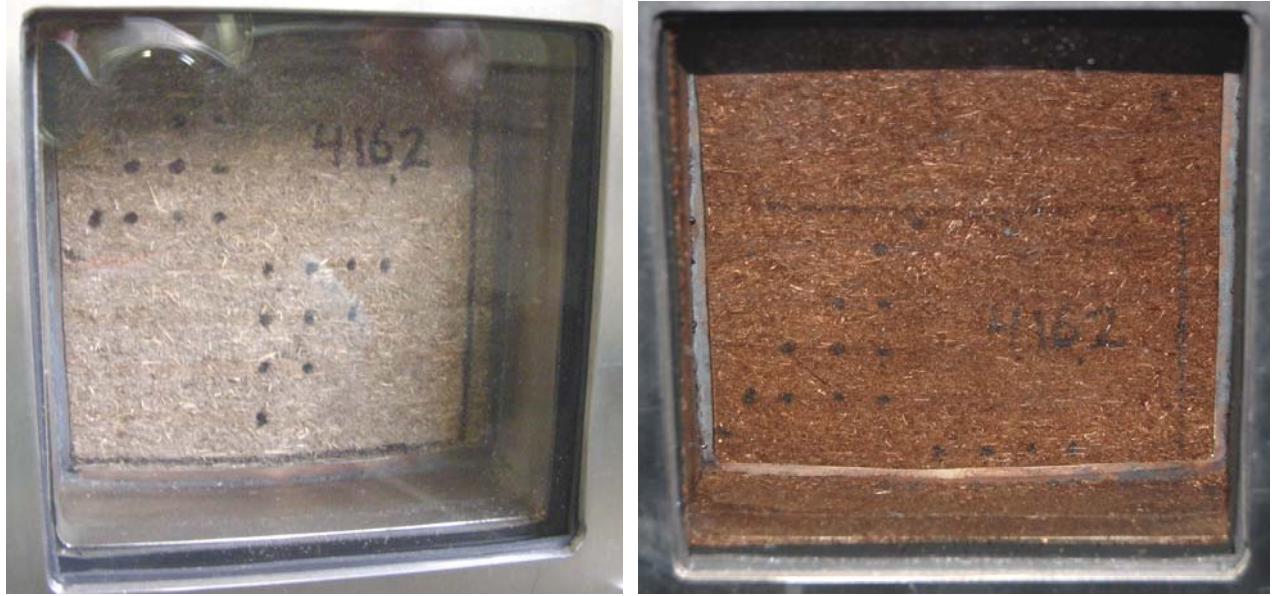


(e) 49 wk



(f) 81 wk

Figure 9. Sequence of photographs of small removable fiberboard sections from test LE2.



(a) baseline (b) after 81 weeks in test
Figure 10. View of the side of test LE2 through the view port

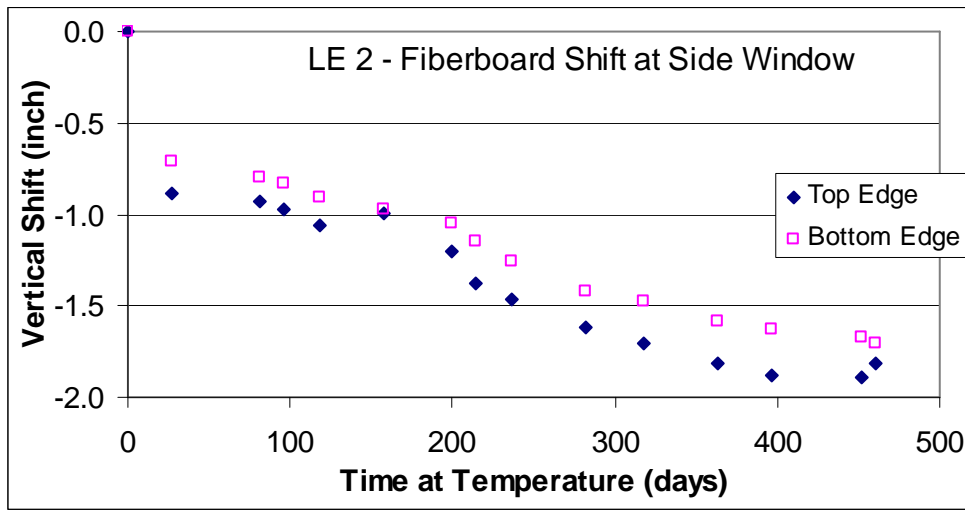


Figure 11. Vertical shift (downward) of fiberboard in LE2, as viewed through the side view port.



Figure 12. LE2 shield with corrosion product after end of test (81 wks)

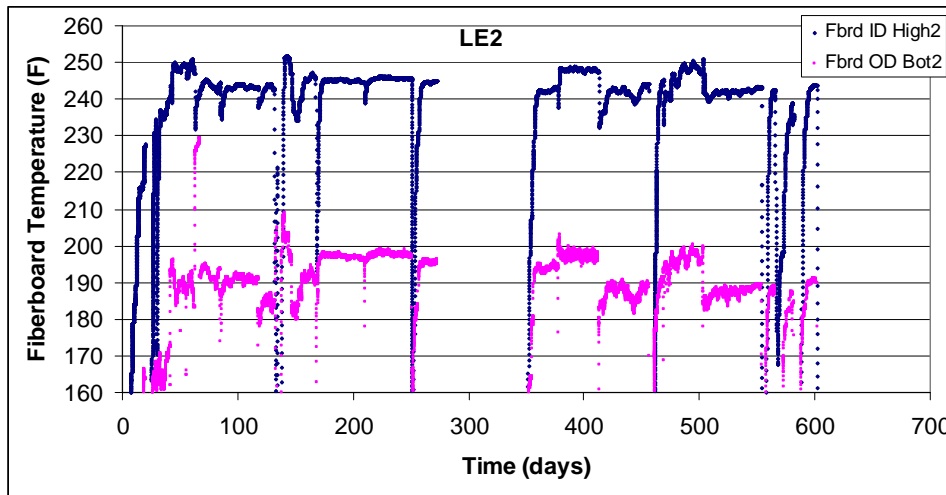


Figure 13. Temperature variation for each package at the hottest (blue symbols) and coolest (pink symbols) instrumented fiberboard locations (highest fiberboard ID location and lowest fiberboard OD location – refer to Figure 1).

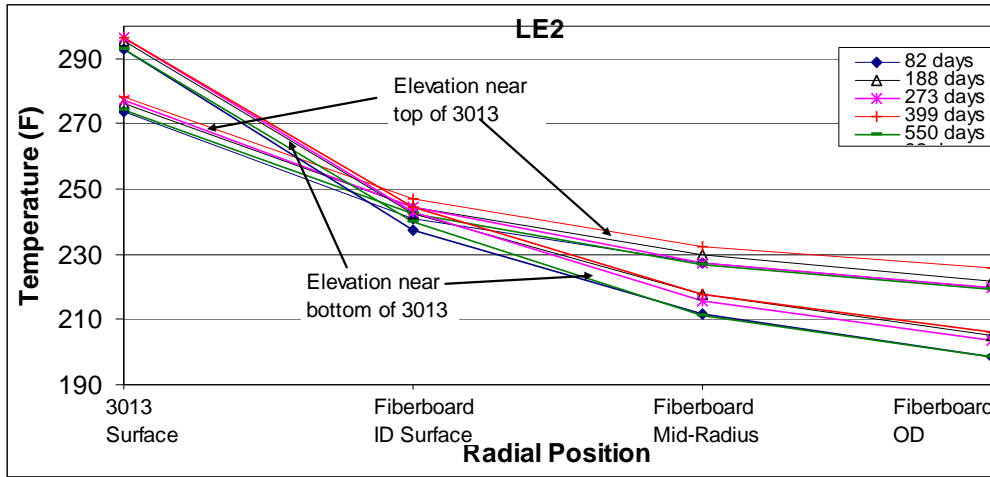


Figure 14. Radial temperature profiles at several intervals of steady state temperature.

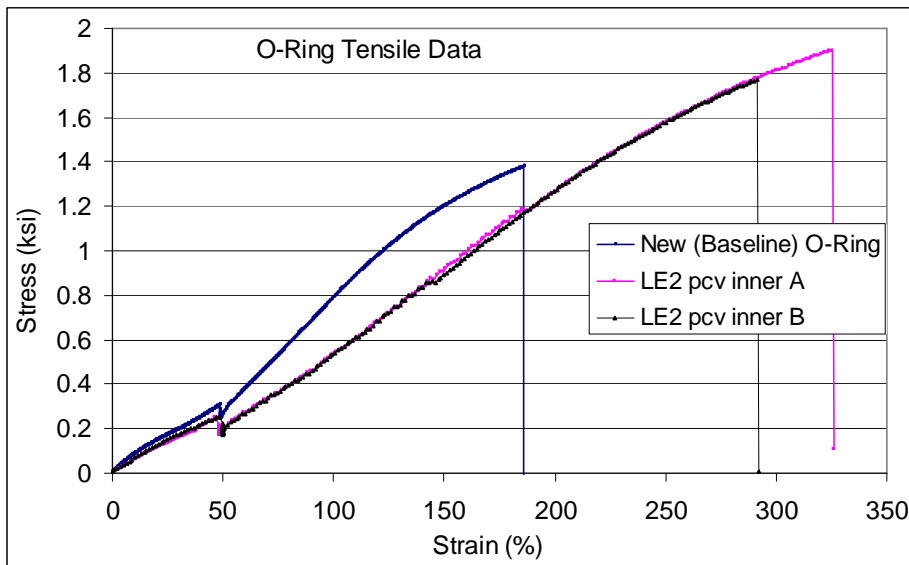


Figure 15. PCV inner O-ring tensile stress-strain curves, compared to non-aged O-ring.

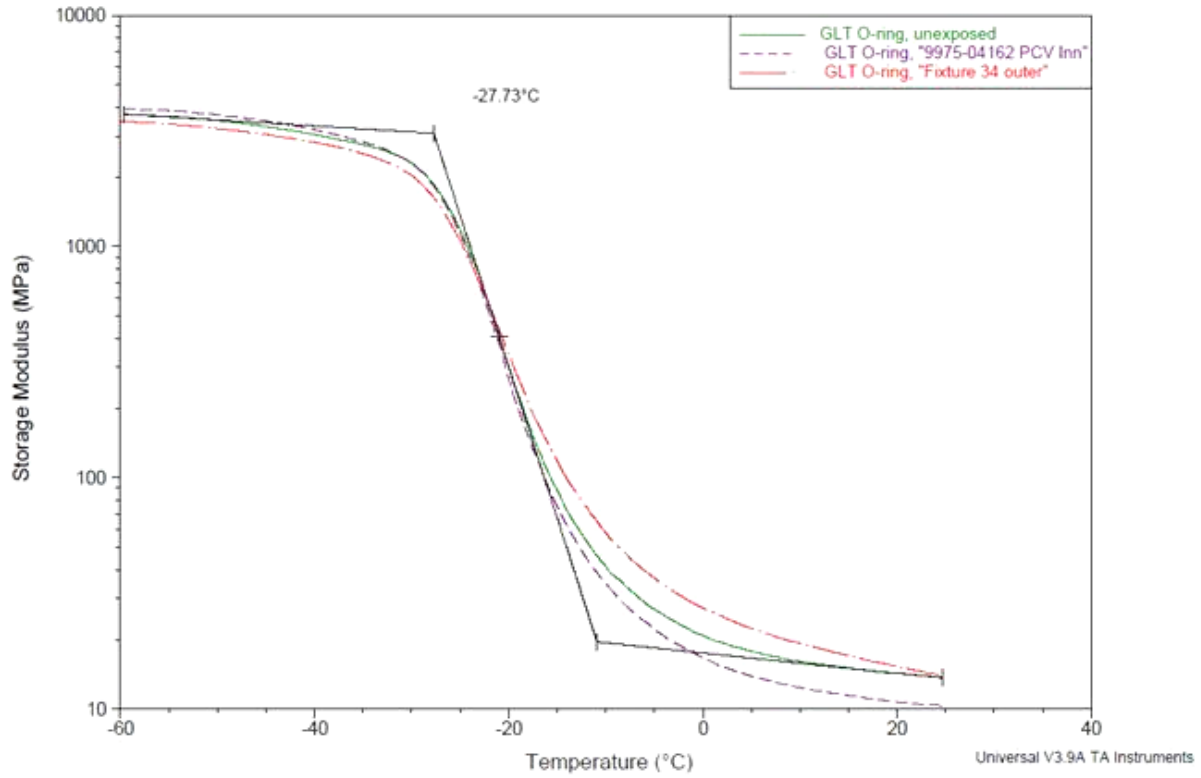
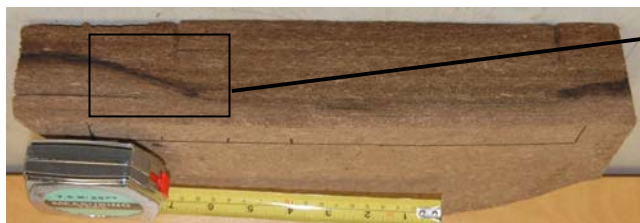


Figure 16. DMA results showing the glass transition temperature for the LE2 PCV inner O-ring. For comparison, results from a non-aged O-ring and an O-ring with a more severe aging history are also shown. The glass transition temperature for each sample was nearly identical, ranging from -27.7 to -28.6C.



(a) OD surface



(b) Internal sectioned surface



(c) Detail of internal surface

Figure 17. Cross section through the bottom layers of the lower fiberboard assembly, showing 3 distinct regions.

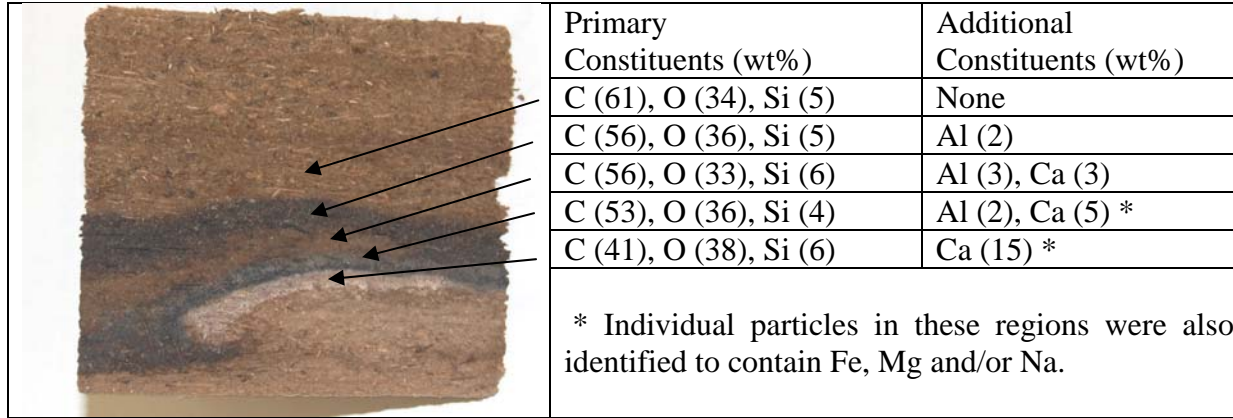


Figure 18. Scanning electron microscope elemental analysis for region near bottom of fiberboard.

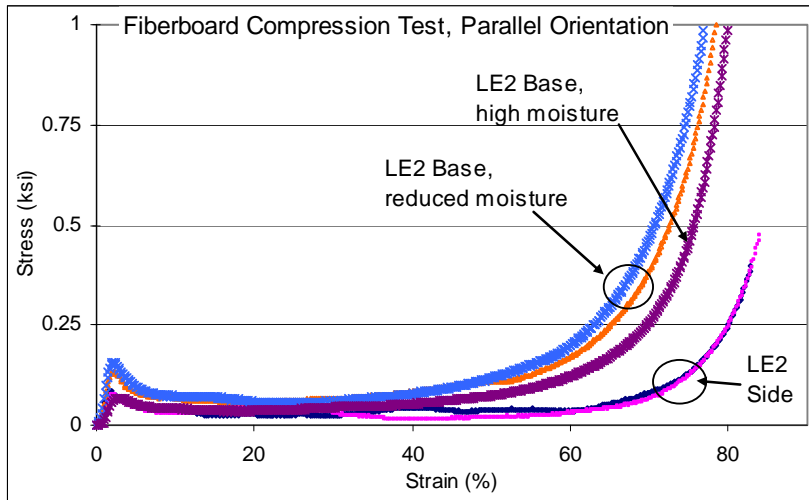


Figure 19. Compression stress-strain curves for LE2 fiberboard samples, parallel orientation.

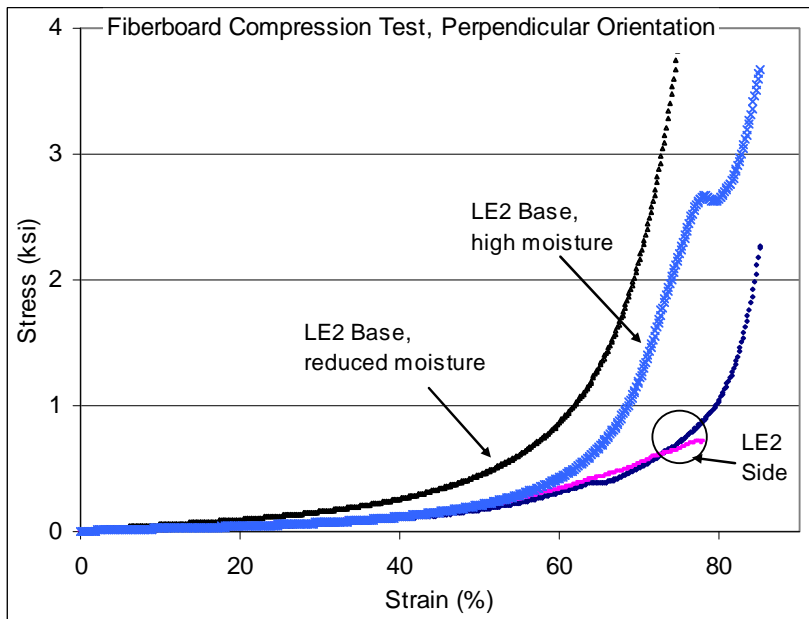


Figure 20. Compression stress-strain curves for LE2 fiberboard samples, perpendicular orientation.

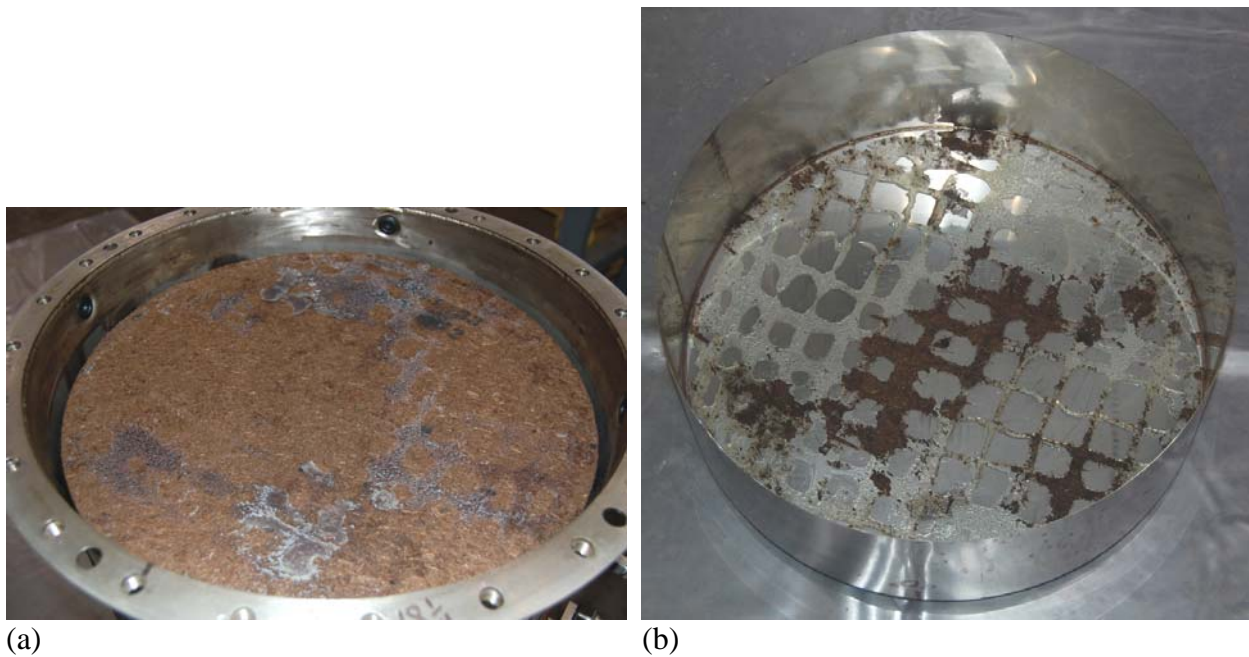


Figure 21. LE2 upper assembly after air shield came loose (a), and underside of air shield (b)

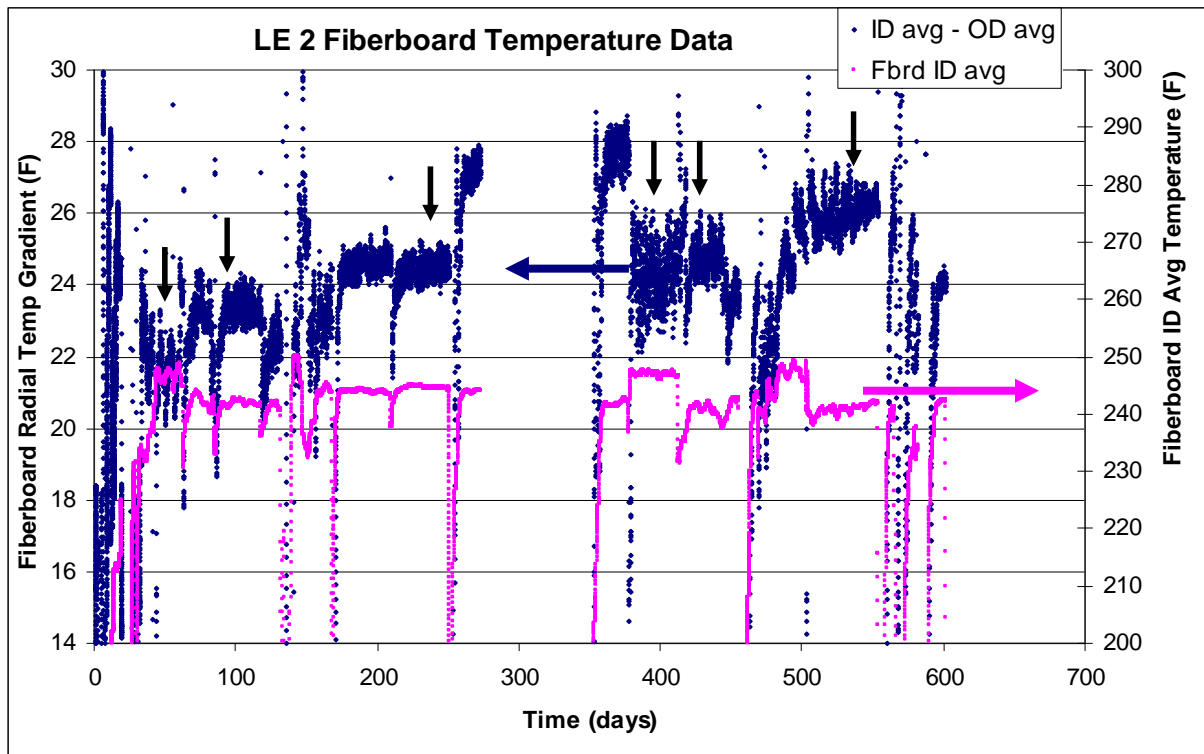


Figure 22. LE package 2 average radial temperature gradient (blue symbols) in the fiberboard based on the upper 3 fiberboard ID thermocouples and the upper 3 fiberboard OD thermocouples, and average fiberboard ID temperature (pink symbols). The vertical arrows indicate times during steady state operation for which the relative thermal conductivity of the fiberboard was estimated.

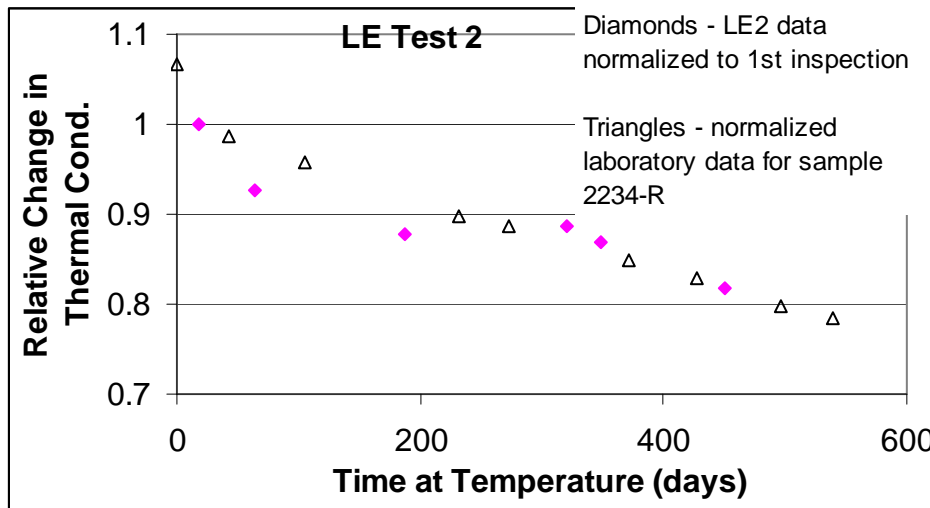


Figure 23. Relative change in radial thermal conductivity estimated from LE2 thermal gradient data, as reported in Reference 6. Comparable data from lab sample 2234-R for a mean test temperature of 185°F following conditioning at 250°F are also shown. These results are superseded by those shown in Figure 24.

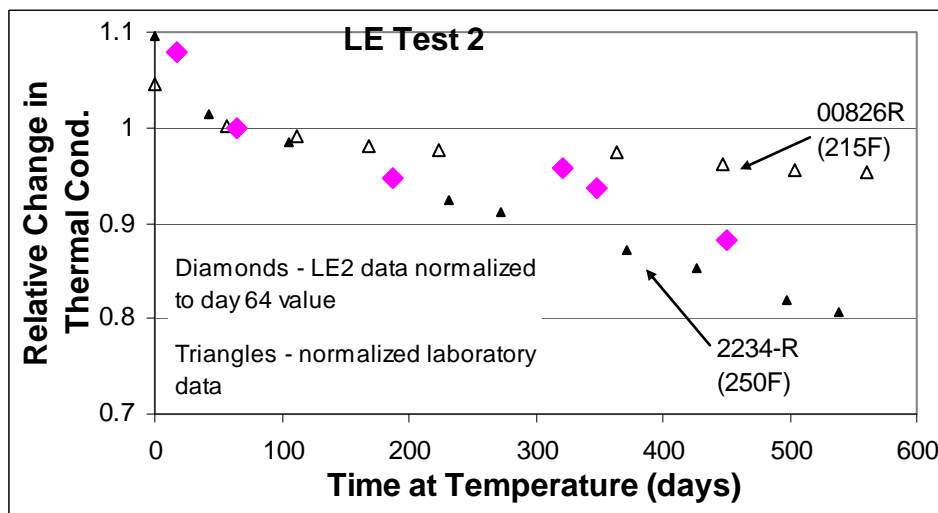


Figure 24. Relative change in radial thermal conductivity estimated from LE2 thermal gradient data, re-normalized to the result for 64 days at temperature. The first data point (following 18 days at temperature) might not meet the assumption of constant heat flux compared to subsequent data points. Comparable data for laboratory samples 2234-R (conditioned at 250°F) and 00826R (conditioned at 215°F) are also shown. The mean test temperature for both laboratory samples was 185°F.

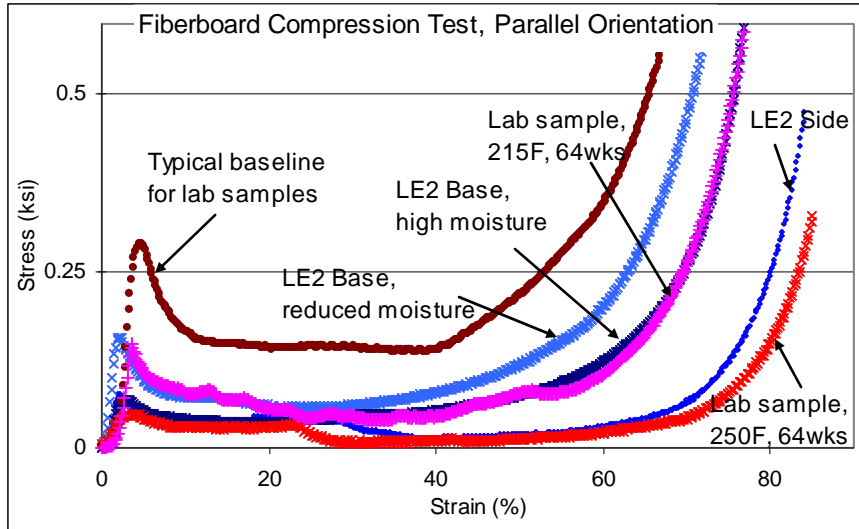


Figure 25. Compression stress-strain curves comparing LE2 fiberboard samples with laboratory samples, parallel orientation.

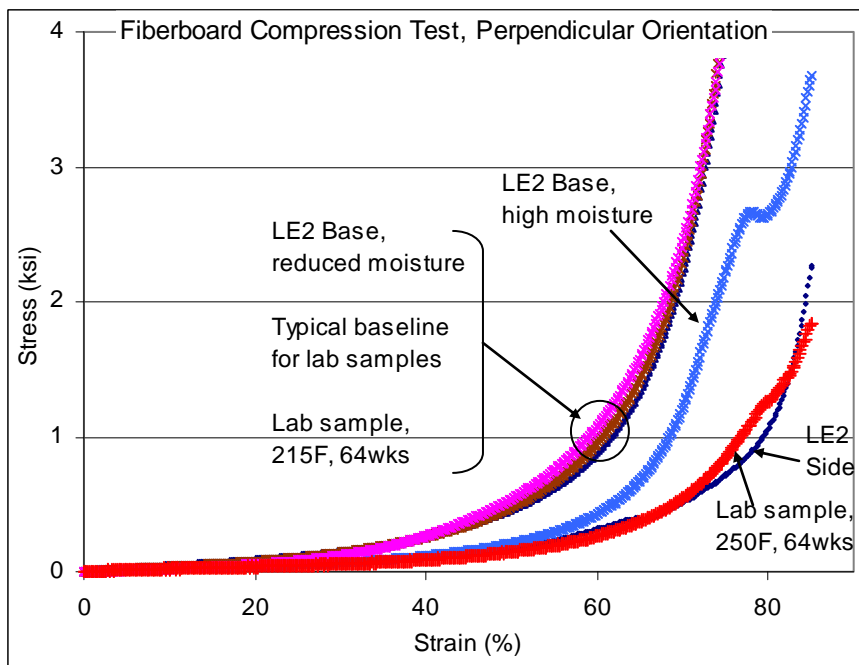


Figure 26. Compression stress-strain curves comparing LE2 fiberboard samples with laboratory samples, perpendicular orientation.

CC:

B. L. Anderson, LLNL, Bldg 1677
J. S. Bellamy, 773-41A
K. P. Burrows, 705-K
G. T. Chandler, 773-A
W. L. Daugherty, 773-A
K. A. Dunn, 773-41A
B. A. Eberhard, 105-K
T. J. Grim, 105-K
E. R. Hackney, 705-K
M. K. Hackney, 705-K
N. C. Iyer, 773-41A
J. W. McClard, 703-H
J. W. McEvoy, 730-4B
T. M. Monahan, 705-K
J. L. Murphy, 773-41A
J. M. Shuler, DOE-HQ EM-63
T. E. Skidmore, 730-A
A.J. Stapf, 717-K
T. M. Stefek, 773-41A
L. E. Traver, 705-K
L. S. Yerger, 705-K
Document Control